PHYSICAL REVIEW E **83**, 060902(R) (2011)

Hydrodynamics of a microhunter: A chemotactic scenario

Ali Najafi*
Department of Physics, Zanjan University, Zanjan 313, Iran
(Received 29 September 2010; published 16 June 2011)

Inspired by biological chemotaxis along circular paths, we propose a hydrodynamic molecular scale hunter that can swim and can find its target. The system is essentially a stochastic low-Reynolds-number swimmer with the ability to move in two-dimensional space and to sense the local value of the chemical concentration emitted by a target. We show that, by adjusting the geometrical and dynamical variables of the swimmer, we can always achieve a swimmer that can navigate and can search for the region with a higher concentration of a chemical emitted by a source.

DOI: 10.1103/PhysRevE.83.060902 PACS number(s): 87.17.Jj, 07.10.Cm, 47.15.G−

Propulsion mechanisms for microorganisms and artificial swimmers are subject to the exceptional constraints of motion in low-Reynolds-number hydrodynamics [1,2]. Purcell's scallop theorem illustrates very well how a set of nonreciprocal body deformations is necessary to achieve a net translational or rotational movement in simple systems [3–10]. Experimental verification of the swimming motion in systems with only a small number of internal degrees of freedom has attracted interest in developing new artificial swimmers [11,12]. Although, in biological systems, many transport phenomena are dominated by diffusion, directed motion is also important. The sperm cell, as a micrometer scale hunter, uses beating flagella to swim toward its targets [13–16]. These targets are the egg cells in the fertilization process. A concentration gradient of the emitted chemical by the source is established in this chemotaxis phenomenon [17]. The physical mechanism of chemotaxis in flagellated cells, such as sperm with circular trajectories is usually described in the following way [18]: The underlying chemical network of an active stimulus-response system provides a concentration mediated stimulus that periodically regulates the internal motion and modulates the curvature of the swimming path. The input in this signaling system is the local value of a chemical [19,20]. This scenario gives rise to a drift in the circular trajectories of chiral flagellated swimmers [18,21].

In this paper, inspired by chemotaxis, we propose a molecular scale swimmer or a hydrodynamic machine that uses the navigation strategy presented in Ref. [18] to move. This machine can navigate in two-dimensional (2D) space, along the gradient of a stimulating chemical. We assume that the chemical can activate a relaxation process in the swimmer and initiate signals which change the internal motion and lead the system to find the right track. We investigate the conditions under which the swimmer can reach the region with higher concentration of the chemical.

Consider a minimal hydrodynamic propeller composed of two large and small spheres with radii R and a, where $a < R$. These spheres are connected through a negligible diameter arm that does not interact with the ambient fluid. Different internal configurations of the system can be achieved by changing the length and shape of the arm. As a specific case, we consider that the arm always stays in a 2D plane, as shown schematically in Fig. 1. For further simplification of the model, we decrease the number of internal configurations to three different states denoted by states (1), (2), and (3). State (1) is a reference state where two spheres are separated by a distance L. States (2) and (3) are characterized by a distance ϵ and an angle Φ with respect to the reference state (1), as depicted in Fig. 1. The small sphere can jump between the denoted states along the shown paths with a constant velocity v_0, measured in the reference frame of the large sphere. A complete cycle of the motion fulfills the Purcell's scallop theorem and eventually leads the system to a new state with a net translational and rotational displacement [2]. The motion is restricted to a 2D plane that is characterized by the plane of the arm. To simplify the description, we further assume that the radius of the small sphere is much smaller than the other length scales of the system, namely, R and L ($a \ll R$, $a \ll L$). In this case, the motion of the small sphere can be regarded as a singular body force located at the position of this sphere. Taking advantage of this simplification and using the linearity of the Stokes equation, we can describe the dynamics of the system for a general internal motion. In the reference frame, which is comoving and rotating with the large sphere, we denote the position vector of the small sphere by $\mathbf{r}_0(t)$. Denoting the linear and angular velocities of the large sphere in a laboratory frame by $\mathbf{V}$ and Ω, we can express the velocity field of the fluid at a general point $\mathbf{r}$ in the comoving frame as

$$\mathbf{u}(\mathbf{r}) = -\mathbf{V} - \Omega \times \mathbf{r} + M \cdot \mathbf{V} + \Omega \times \mathbf{m} + G(\mathbf{r},\mathbf{r}_0) \cdot \mathbf{f}, \quad (1)$$

where $\mathbf{f}$ denotes the strength of the point force located at the position of the small sphere. Here, the tensor M and the vector $\mathbf{m}$ give the flow field due to the translational and rotational motions of a moving sphere and are given explicitly as $M = \frac{3}{4}\frac{R}{r}(\mathbf{I} + \frac{\mathbf{rr}}{r^2}) + \frac{1}{4}\frac{R^3}{r^3}(\mathbf{I} - 3\frac{\mathbf{rr}}{r^2})$ and $\mathbf{m} = \frac{R^3}{r^3}\mathbf{r}$. The Green's function of the Stokes equation for an infinite flow bounded internally by a solid sphere with radius R is denoted by $G(\mathbf{r},\mathbf{r}_0)$. The explicit form of this Green's function has been calculated by Oseen [22]. Force and torque balances of a self propeller system require that the total force and torque acting on the fluid must vanish. The point force located near the sphere has an image force with strength $\mathbf{f}_i = (c_1\hat{\mathbf{r}}_0\hat{\mathbf{r}}_0 + c_2\mathbf{I}) \cdot \mathbf{f}$ with $c_1 = -\frac{3}{4}(\frac{R}{r_0} - \frac{R^3}{r_0^3})$ and $c_2 = -\frac{3}{4}\frac{R}{r_0} - \frac{1}{4}\frac{R^3}{r_0^3}$, and $\mathbf{I}$ is the unit matrix. This image force is located inside the sphere in the

*najafi@znu.ac.ir

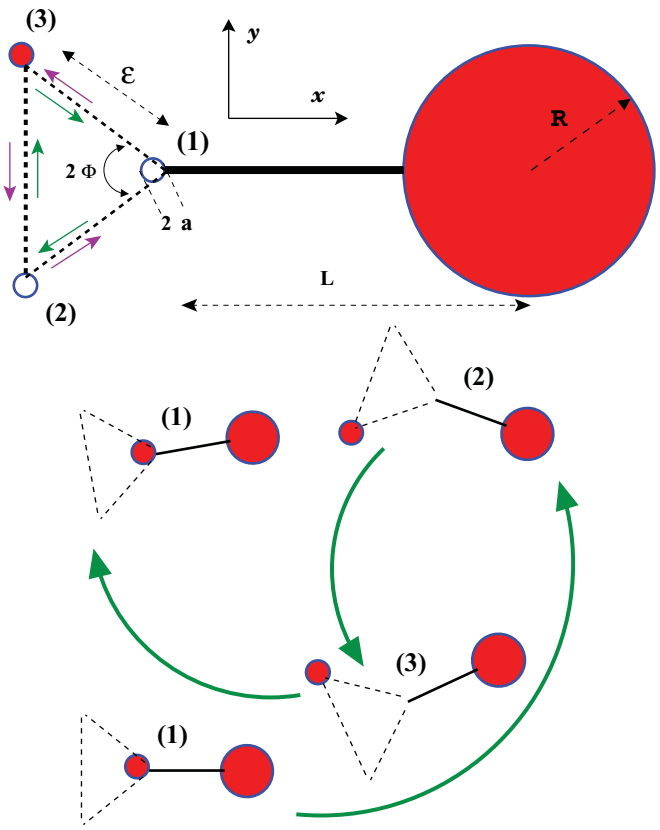

FIG. 1. (Color online) Two large and small spheres are connected through an arm to construct a swimmer that can move in 2D space. In a stochastic description of the motion, we assume that the small sphere can be in one of the three distinct states as shown in the picture.

position given by $\mathbf{r}_0^* = \frac{R^2}{r_0^2}\mathbf{r}_0$. A discussion by Higdon shows that, in an evaluation of the force acting on the fluid, one should carefully account for the image system [23]. In this case, the force and torque balances read as follows:

$$\mathbf{f} + \mathbf{f}_i + 6\pi\eta R\mathbf{V} = 0, \qquad \mathbf{r}_0 \times \mathbf{f} + \mathbf{r}_0^* \times \mathbf{f}_i + 8\pi\eta R^3\Omega = 0.$$

To finish with the dynamical equations, we should include the prescribed form of the internal motion by the boundary condition $\mathbf{u}(\mathbf{r}_0) = \dot{\mathbf{r}}_0$. By having the force balance equations and this boundary condition in hand, we can eliminate the point force strength and can arrive at equations for linear and angular velocities of the system and can obtain the velocity of the large sphere as $\mathbf{V} = \mathbf{A}\cdot\dot{\mathbf{r}}_0$ and $\Omega = \mathbf{B}\cdot\dot{\mathbf{r}}_0$, where $\mathbf{A}$ and $\mathbf{B}$ are two matrices in which the elements strongly depend on the specific form of the internal motion given by function $\mathbf{r}_0(t)$ [24]. We denote the dynamical variables of the system by $\mathbf{x}$ and θ, where $\mathbf{x}$ stands for the position vector of the large sphere and θ measures the angle that the swimmer's director makes with the x axis. The swimmer's director is defined as a unit vector pointing from the position of reference state (1) to the center of the large sphere. Note that $\dot{\mathbf{x}} = \mathbf{V}$, $\dot{\theta} = \Omega$. Now, the differential changes of the swimmer's variables in a general jump from state (i) to state (j) can be written as

$$\Delta\mathbf{x}_{ij} = \mathbf{R}^{-1}(\theta)\cdot\mathbf{d}_{ij}, \qquad \Delta\theta_{ij} = \alpha_{ij}, \tag{2}$$

where $\mathbf{R}(\theta)$ represents the matrix for a rotation around the z axis by the instantaneous value of angle θ. Let us consider the case where the internal deformations are small, compared to the average length of the swimmers, that is, $\epsilon \ll L$. This allows us to set up a perturbative expansion of the results. Up to the leading order in ϵ and a, the differential rotations read as follows:

$$\alpha_{12} = -\frac{3}{4}\left(\frac{\epsilon}{R}\right)\left(\frac{a}{R}\right)\left(1+\frac{L}{R}\right)\sin\Phi,$$
$$\alpha_{23} = \frac{3}{2}\left(\frac{\epsilon}{R}\right)\left(\frac{a}{R}\right)\left(1+\frac{L}{R}\right), \tag{3}$$

and $\alpha_{31} = \alpha_{12}$. For the leading order in ϵ and a, the displacement vectors read as follows:

$$\mathbf{d}_{12} = \begin{pmatrix}\delta_1\\ \delta_2\end{pmatrix}, \quad \mathbf{d}_{23} = \begin{pmatrix}0\\ \delta_3\end{pmatrix}, \quad \mathbf{d}_{31} = \begin{pmatrix}-\delta_1\\ \delta_2\end{pmatrix}, \tag{4}$$
$$\delta_1 = \epsilon\frac{a}{R}\left(1-\frac{3}{2}\frac{R}{L}\right)\cos\Phi, \quad \delta_2 = \epsilon\frac{a}{R}\left(1-\frac{3}{4}\frac{R}{L}\right)\sin\Phi,$$

and $\delta_3 = -4\delta_2$. The results are given for $R \ll L$. The scallop theorem allows us to simply express the changes for reverse jumps in terms of the forward jumps such that $\Delta\mathbf{x}_{ji} = -\Delta\mathbf{x}_{ij}$ and $\Delta\theta_{ij} = -\Delta\theta_{ji}$. We have assumed that all jumps happen with a constant velocity v_0. In this case, the time required for jump $1 \to 2$ $(3 \to 1)$ is equal to $\tau_1 = \epsilon/v_0$ $(\tau_3 = \epsilon/v_0)$, and the time for jump $2 \to 3$ is equal to $\tau_2 = 2\sin\Phi\epsilon/v_0$. The trajectory of the motion for the swimmer moving in a cyclic way $(1 \to 2 \to 3 \to 1)$ is a circular path with the curvature given by $\kappa_0^{-1} = (2\delta_2 + \delta_3)$.

To construct the stochastic model, we denote the probability of the system to be in state (i) by P_i. The transition rate for stochastic jump from state (i) to state (j) is denoted by ω_{ij}. The rates for the internal conformational changes, in general, depend on the temperature of the fluid and the detailed internal activity of the system. The dynamics of this stochastic system is governed by the Fokker-Planck equations as $\dot{P}_1 = \omega_{31}P_3 + \omega_{21}P_2 - (\omega_{12}+\omega_{13})P_1$ and $\dot{P}_2 = \omega_{32}P_3 + \omega_{12}P_1 - (\omega_{21}+\omega_{23})P_2$, where the dot symbol denotes the time derivative; also note that the probability conservation implies that $P_1 + P_2 + P_3 = 1$. The differential change of the displacement per unit time for this stochastic system at a mean field level can be written as

$$\frac{d\mathbf{x}}{dt} = P_1(\omega_{12}\Delta\mathbf{x}_{12} + \omega_{13}\Delta\mathbf{x}_{13}) + P_2(\omega_{23}\Delta\mathbf{x}_{23} + \omega_{21}\Delta\mathbf{x}_{21}) + P_3(\omega_{31}\Delta\mathbf{x}_{31} + \omega_{32}\Delta\mathbf{x}_{32}),$$

and a similar equation for the rate of change of θ while we replace all $\Delta\mathbf{x}_{ij}$'s with α_{ij}. For a system that is in the thermodynamic equilibrium, the transition rates for all jumps are symmetric $(\omega_{ij} = \omega_{ji})$, and the time average velocity of this system is zero. If, for any reason, the detailed balance violates the internal conformational changes, the system will behave like a circle swimmer. As an example, let us assume that the rates for all clockwise jumps are equal such that $\omega_{12} = \omega_{23} = \omega_{31} = \omega_0$ and all the other counterclockwise jumps are set to $\omega_0 + \delta\omega$. In this case and for small $\delta\omega$, the trajectory is a circle with the radius of curvature given by $\kappa^{-1} = (\delta\omega/\omega_0)\kappa_0^{-1}$, where we have already defined κ_0.

Now, let us consider a fluid medium occupied by a very low concentration of chemical attractants given by $\rho(\mathbf{x})$. The low concentration assumption makes sure that the hydrodynamic properties of the medium are not affected by this chemical. This chemical can drive the system into a nonequilibrium concentration by affecting the internal conformational changes. Inspired by the chemotactic navigation in biological microorganisms, we assume that there is a density sensing mechanism in the system. In the signaling network of the chemotactic systems, a dynamical mechanism is capable of producing an output signal that depends on the time history of the stimulating properties. Local concentration of the chemoattractants is the stimulating property in this case. Mathematics of this adaptation mechanism can be modeled by a relaxational process [18,25]. In this model, an internal adaptation variable $u(t)$ couples to a signaling function $s(t)$ through the following equations:

$$\sigma \dot{s} = \rho u - s, \qquad \mu \dot{u} = u(1 - s), \tag{5}$$

where the adaptation variable u measures the dynamical sensitivity with the time scale of adaptation given by μ. The relaxational process in a time scale controlled by σ will produce a stimulus $s(t)$ that can affect the dynamical variables of the conformational changes that are already defined by ω_{ij}. As an example, we consider an active swimmer with a circular trajectory where all the counterclockwise rates are different from the clockwise rates by a factor of r as $\omega_{ccw} = r\omega_{cw} = r\omega_0$. Now, we assume that the adaptation mechanism controls only one of the rates as $\omega_{13} = s(t)r\omega_0$. Here, $r \neq 1$ sets an asymmetry for the swimmer and drives it out of equilibrium where, for a uniform profile of the concentration, the system reaches a steady state with $s = 1$ that is a circle swimmer. Now, we can investigate the response of a circling swimmer, embedded in a gradient of chemical concentration. Figure 2 (left) shows a typical trajectory for the swimmer moving in a linear gradient of chemical concentration given by $\rho(\mathbf{x}) = a_1 + a_2 x$. A typical trajectory of the swimmer for motion in an environment occupied by a central gradient given by $\rho(\mathbf{x}) = a_3/|\mathbf{x}|$, with $a_3 > 0$ is presented in Fig. 2 (right).

The different trajectories of the swimmer look like a circle with a drifting center. For a linear gradient of concentration, the overall drift lies along a straight line that makes an angle ψ with respect to the direction of the gradient. This angle

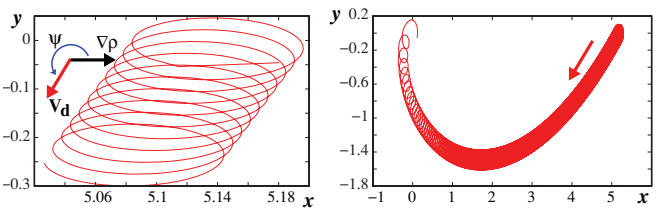

FIG. 2. (Color online) Two different trajectories for the swimmer moving in a linear, left, and a central, right, gradient of the chemical concentration. In the left example, angle ψ discriminates different outcomes of the motion: motion toward the higher or lower concentration. Parameters in both graphs are given by $R = 1, \omega_0 = 1$, $a = 0.2$, $L = 6.1$, $\epsilon = 0.6$, $a_1 = 20$, $a_2 = 1$, $a_3 = 8$, $\sigma = 0.1$, and $\mu = 10$, for the left graph, $\Phi = \pi/12$, $r = 5$, while for the right graph, $\Phi = \pi/6$, $r = 10$.

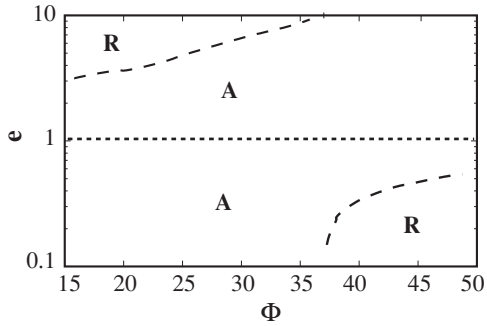

FIG. 3. Different behaviors of the trajectories in a linear concentration, categorized in a phase diagram. The horizontal axis Φ stands for a geometrical variable of the system, and the vertical axis shows r, the anisotropy parameter that makes the individual swimmer an active system. Drifting trajectories going toward the region with higher (lower) concentration, are denoted by A (R).

discriminates the states moving toward the higher or lower values of the concentration. For a slowly varying concentration and for the above example, a perturbation analysis shows that the drift direction reads as follows: $\tan\psi = -\tan(\theta_1 + \theta_2)$, where as shown in Ref. [18], the phase lag between the signaling function $s(t)$ and the trajectory oscillations θ_1 involves discriminating the trajectories and $\tan\theta_2 = [\Omega^2(2 + r) + 3 + 9r + 9r^2 + 6r^3]/[\Omega^3 + 3\Omega r(2 + r)]$. Here, the dimensionless frequency (with ω_0) of the oscillations is given by $\Omega = (1/2)(r - 1)(a/R)(\epsilon/R)(1 + L/R)(1 - \sin\Phi)$.

Interestingly, all the results are independent of the initial orientations of the swimmer. To get a better feeling for the results, we summarize the different trajectories in a linear gradient of a chemical in a phase diagram presented in Fig. 3. In this phase diagram, attractive states in the regions with higher concentration and repulsive states from the higher concentrations are denoted by the labels (A) and (R), respectively. The horizontal axis Φ shows the geometrical variable of the system, and the vertical axis r is the asymmetric parameter that makes the individual swimmer an active system. For $r = 1$, the swimmer is not moving, but for $r \neq 1$, we have an active circle swimmer that can respond to the chemical concentration. This picture shows that, for an active system (a system that can move in a uniform concentration), by adjusting the parameters, it is always possible to construct a swimmer that can navigate in the correct direction.

Here, we should emphasize that our model captures the features presented in a generic description of Ref. [18] and goes beyond that description by introducing a specific detailed hydrodynamic structure that takes the interplay between the geometry of the swimmer and the conformational rates into account (Fig. 3). This proposed system could, in principle, be realized artificially by synthesizing a molecular machine from proteins with allosteric interactions that possess sensitivity in their conformations [26]. From the biophysical world, such drifting trajectories are being observed for sea urchin sperm cells [19], but one should note that, in the bacterial propulsion, the stochastic turning events are infrequent ($\sim$0.1–1 Hz) and can change the swimming direction. Here, we have neglected the effects of thermal noise. The validity of this assumption requires that the displacement, during a typical jump due to

the thermal fluctuations, should be less than the swimming displacement. This condition can be translated as a criterion for the time of the jumps. Denoting the thermal energy by k_BT, we see that the thermal noise can be neglected for transition rates that satisfy $\omega_{ij}^{-1} \ll (6\pi\eta/k_BT)(\epsilon^2 a^2/R)$. For a micrometer size system with $a \sim \epsilon \sim 0.1R$ that works in water, the effects of thermal noise at room temperature are negligible for $\omega_{ij} \gg 10^3\ \mathrm{s}^{-1}$. In a concentration gradient, the force due to the nonequilibrium concentration is also important [27]. Here, we have neglected the effects due to this force. A dimensional analysis shows that, for satisfying this condition, the following criterion must hold: $|\nabla\rho| \ll \omega_0(a\epsilon\eta)/(R^3 k_BT)$, where ω_0 is a typical value for the rates of conformational changes.

In conclusion, we have introduced a micrometer scale system that uses the physics of biological chemotaxis to navigate along a preferred direction into a source.

I thank M. Bazargan and F. Mohammad-Rafiee for reading the manuscript and acknowledge support from the MPIPKS. I also thank B. M. Friedrich for useful comments.

[1] E. Lauga and T. R. Powers, Rep. Prog. Phys. **72**, 096601 (2009).
[2] E. M. Purcell, Am. J. Phys. **45**, 3 (1977).
[3] J. E. Avron, O. Gat, and O. Kenneth, Phys. Rev. Lett. **93**, 186001 (2004).
[4] L. E. Becker, S. A. Kochler, and H. A. Stone, J. Fluid Mech. **490**, 15 (2003).
[5] R. Dreyfus, J. Baudry, and H. A. Stone, Eur. Phys. J. B **47**, 161 (2005).
[6] D. Tam and A. E. Hosoi, Phys. Rev. Lett. **98**, 068105 (2007).
[7] C. M. Pooley, G. P. Alexander, and J. M. Yeomans, Phys. Rev. Lett. **99**, 228103 (2007).
[8] A. Najafi and R. Golestanian, J. Phys.: Condens. Matter **17**, S1203 (2005); R. Zargar, A. Najafi, and M.-F. Miri, Phys. Rev. E **80**, 026308 (2009).
[9] B. U. Felderhof, Phys. Fluids **18**, 063101 (2006).
[10] S. Günther and K. Kruse, Europhys. Lett. **84**, 68002 (2008).
[11] E. R. Kay, D. A. Leigh, and F. Zerbetto, Angew. Chem., Int. Ed. **46**, 72 (2007); R. Dreyfus *et al.*, Nature (London) **437**, 862 (2005); M. Leoni *et al.*, Soft Matter **5**, 472 (2009).
[12] W. F. Paxton *et al.*, Angew. Chem., Int. Ed. **45**, 5420 (2006); J. Am. Chem. Soc. **126**, 13424 (2004); S. Fournier-Bidoz *et al.*, Chem. Commun. (Cambridge), 441 (2005); N. Mano and A. Heller, J. Am. Chem. Soc. **127**, 11574 (2005); R. Golestanian, T. B. Liverpool, and A. Ajdari, Phys. Rev. Lett. **94**, 220801 (2005).
[13] I. H. Riedel *et al.*, Science **309**, 300 (2005).
[14] D. Bray, *Cell Movements: From Molecules to Motility*, 2nd ed. (Garland, New York, 2001).
[15] R. L. Miller, *Biology of Fertilization*, Vol. 2, edited by C. B. Metz and A. Monroy (Academic, New York, 1985), pp. 275–337. M. Eisenbach and L. C. Giojalas, Nature Reviews Molecular Cell Biology **7**, 276 (2006).
[16] H. C. Berg and D. A. Brown, Nature (London) **239**, 500 (1972).
[17] H. C. Berg, *E. coli in Motion* (Springer-Verlag, New York, 2004).
[18] B. M. Friedrich and F. Jülicher, New J. Phys. **10**, 123025 (2008); Proc. Natl. Acad. Sci. U.S.A. **104**, 13256 (2007).
[19] U. B. Kaupp *et al.*, Nat. Cell Biol. **5**, 109 (2003); U. B. Kaupp, N. D. Kashikar, and I. Weyand, Annu. Rev. Physiol. **70**, 93 (2008).
[20] T. Strünker *et al.*, Nat. Cell Biol. **8**, 1149 (2006).
[21] R. Thar and T. Fenchel, Appl. Environ. Microbiol. **67**, 3299 (2001).
[22] C. W. Oseen, *Neuere Methoden und Ergebniss in der Hydrodynamik* (Akademishe Verlagsgesellschaft, Leipzig, 1927).
[23] J. J. L. Higdon, J. Fluid Mech. **90**, 685 (1979).
[24] A. Najafi and R. Zargar, Phys. Rev. E **81**, 067301 (2010).
[25] N. Barkai and S. Leibler, Nature (London)**387**, 913 (1997).
[26] J. M. Berg, J. L. Tymoczko, and L. Stryer, *Biochemistry* (Freeman, New York, 2002).
[27] U. M. Córdova-Figueroa and J. F. Brady, Phys. Rev. Lett. **100**, 158303 (2008); F. Jülicher and J. Prost, Eur. Phys. J. E **29**, 27 (2009).